Research Square

Preprints are preliminary reports that have not undergone peer review.
They should not be considered conclusive, used to inform clinical practice,
or referenced by the media as validated information.

Surface engineering of PDMS using gelatin-polyvinyl alcohol for renal cell-compatible microfluidic applications

Upasana Gupta
Indian Institute of Technology Jammu
Shashank Kumar Singh
Indian Institute of Integrative Medicine
Ravi Kumar Arun
ravi.arun@iitjammu.ac.in

Indian Institute of Technology Jammu

Research Article

Keywords: Gelatin-polyvinyl alcohol, PDMS, surface engineering, microfluidics, renal cell carcinoma, wall shear stress, drug response

Posted Date: November 13th, 2026

DOI: https://doi.org/10.21203/rs.3.rs-11351244/v1

License: This work is licensed under a Creative Commons Attribution 4.0 International License.
Read Full License

Additional Declarations: No competing interests reported.

Surface engineering of PDMS using gelatin-polyvinyl alcohol for renal cell-compatible microfluidic applications

Upasana Gupta[1], Shashank Kumar Singh[2*], Ravi Kumar Arun[1*]

[1]Department of Chemical Engineering, Indian Institute of Technology Jammu, Jammu and Kashmir, India,181221
[2]Council of Scientific and Industrial Research-Indian Institute of Integrative Medicine, Jammu, Jammu and Kashmir, India, 180001

* Corresponding author Email: ravi.arun@iitjammu.ac.in

Abstract

The development of a microfluidic biointerface that supports different renal-derived cell conditions while maintaining a defined flow environment could improve comparative in vitro drug-response studies. In this study, a gelatin-polyvinyl alcohol (gelatin-PVA)-modified poly(dimethylsiloxane) (PDMS) microfluidic platform was developed as a proof-of-concept system for renal cell culture and future comparative therapeutic evaluation. A three-channel device was fabricated with two lateral culture channels and a central channel intended for controlled fluid or drug delivery. Gelatin, PVA, and gelatin-PVA coatings were first evaluated on planar PDMS substrates. The combined gelatin-PVA coating reduced the apparent water contact angle from approximately 115° on untreated PDMS to approximately 74° and supported favorable attachment, spreading, and metabolic activity of A498 renal carcinoma and HEK-293 renal-derived comparison cells under plate-based conditions. The selected coating was subsequently applied to the microfluidic device. Dye-flow testing confirmed continuous channel filling without visible leakage. Based on the reported channel dimensions (700 μm width and 150 μm height) and an imposed flow rate of 10 μL min^{-1}, analytical hydrodynamic estimates gave a mean velocity of approximately 1.59 mm s^{-1}, a hydraulic diameter of approximately 247 μm, a Reynolds number of approximately 0.42, and a nominal wall shear stress of approximately 0.059 Pa (0.59 dyn cm^{-2}), using a literature viscosity of 0.93 mPa s for DMEM containing 10% fetal bovine serum at 37 °C. These values indicated a low-Reynolds-number laminar-flow regime. A498 cells were successfully introduced into the coated microchannels, and qualitative live/dead fluorescence imaging showed calcein-positive cells with no visible propidium iodide signal in the representative fields. Plate-based 5-fluorouracil and hydroxychloroquine studies provided baseline comparative drug-

sensitivity data for future on-chip evaluation. The study, therefore, established a material, biological, and quantitatively defined fluidic basis for further development of a comparative renal microfluidic platform.

Keywords: Gelatin-polyvinyl alcohol; PDMS; surface engineering; microfluidics; renal cell carcinoma; wall shear stress; drug response

1. Introduction

Renal cell carcinoma (RCC) represents the most common form of kidney cancer and is characterized by substantial biological heterogeneity, altered cellular metabolism, high vascularization, and variable therapeutic response (Mieville et al. 2023). Although targeted therapies, immunotherapies, and combination treatments have improved RCC management, differences in treatment sensitivity and off-target toxicity remain important challenges. During preclinical drug evaluation, anticancer efficacy and toxicity toward non-cancerous renal cells are generally investigated in separate culture systems. Consequently, direct comparison of cancer-cell inhibition and normal-cell damage under equivalent treatment conditions remains difficult. An experimental platform that allows cancerous and non-cancerous renal cell models to be maintained in spatially separated compartments while receiving controlled therapeutic exposure could therefore support more informative evaluation of drug efficacy and cellular toxicity (DesRochers et al. 2014; Soo et al. 2018).

Conventional two-dimensional cell culture has been widely used in cancer research because it is simple, inexpensive, reproducible, and compatible with routine biological assays. However, cells grown under static conditions are not exposed to several important features of the in vivo environment, such as continuous fluid movement, nutrient transport, waste removal, chemical gradients, and fluid-induced mechanical stimulation (Kaur et al. 2025; Zhang et al. 2026). As a result, cell attachment, morphology, metabolism, proliferation, and response to therapeutic compounds may differ from those observed under more physiologically relevant conditions. Animal models can reproduce a more complex biological environment, but they are costly, time-consuming, ethically sensitive, and may not always predict human responses due to interspecies differences (Barré-Sinoussi and Montagutelli 2015; Das et al. 2026). For these reasons, there is

increasing interest in developing controlled in vitro platforms that can combine biological testing with more defined transport and flow conditions.

Microfluidic systems offer several advantages for this purpose. They allow precise handling of small fluid volumes and controlled delivery of culture medium, drugs, and other biochemical factors (Das and Prajapati 2025; Zhang et al. 2025; Mirlohi et al. 2026). Multiple channels can also be incorporated into a single device so that different cell populations can be maintained in separate regions and observed in parallel. Such an arrangement could be useful for comparing the response of renal cancer cells with that of a noncancerous renal-derived cell model under identical treatment conditions. In the proposed design, one compartment could be used for RCC cells, while another could contain non-cancerous comparison cells. A central channel could then be used for controlled delivery of medium or therapeutic compounds. This type of configuration could reduce variation that arises when the two cell conditions are tested separately and could provide a practical way to compare anticancer activity with potential toxicity to non-cancerous cells. Before such a dual-cell platform can be established, however, two conditions must be addressed: the device material must support suitable cell attachment and growth, and the imposed flow conditions must be quantitatively defined because velocity, shear stress, hydraulic resistance, and residence time can influence cellular behavior and therapeutic exposure.

Poly(dimethylsiloxane) (PDMS) is commonly used for the fabrication of microfluidic devices because it is transparent, flexible, gas permeable, and compatible with soft-lithography-based fabrication methods (McDonald and Whitesides 2002; Lima 2025). Its optical transparency is especially useful for observing cells and fluid movement inside closed microchannels. Despite these advantages, untreated PDMS is naturally hydrophobic due to the methyl groups on its surface. This poor wettability can affect how proteins in the culture medium interact with the surface, leading to uneven cell attachment, limited spreading, and changes in cellular morphology (Chumbimuni-Torres et al. 2011; Gokaltun et al. 2017). This becomes particularly important when two different cell models are intended to be cultured in the same device, because the same PDMS surface must support both cellular conditions.

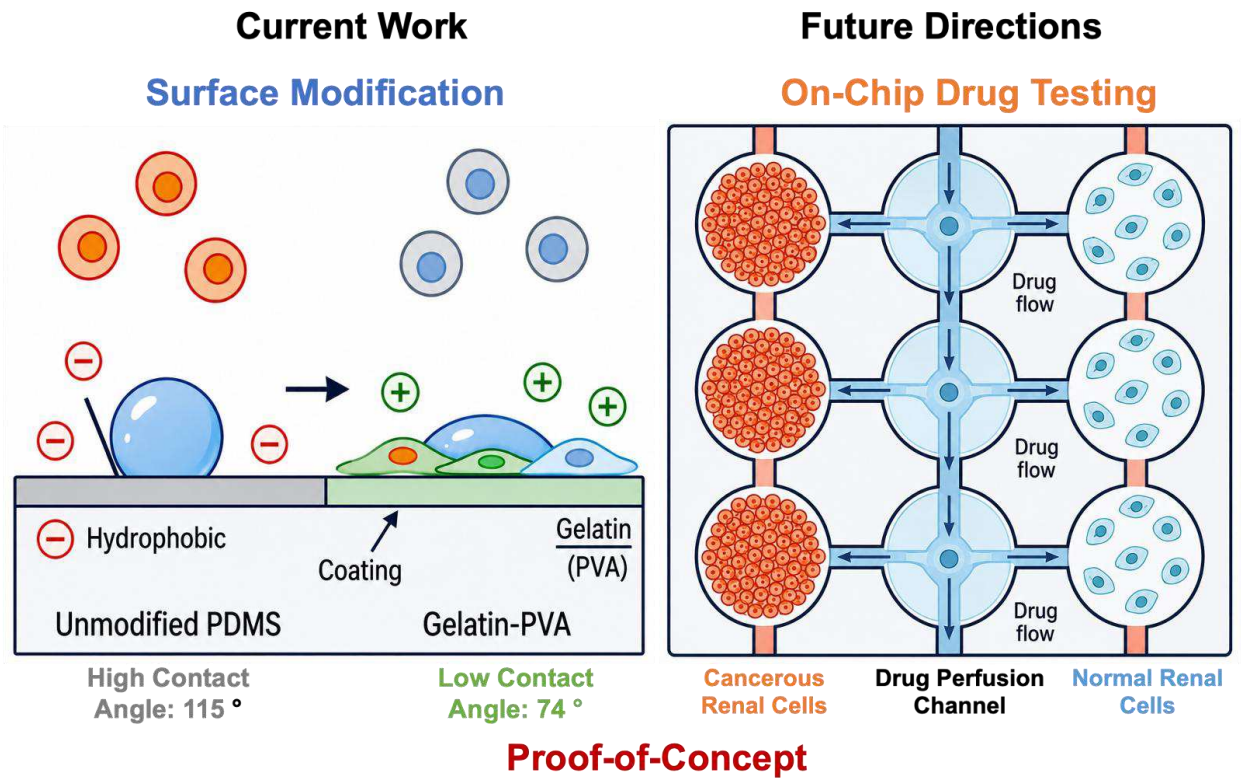


Fig. 1. A proof-of-concept representation of the gelatin-PVA-modified PDMS microfluidic platform for future comparative evaluation of renal drugs.

Surface modification provides a practical approach for improving the interaction between PDMS and biological systems. Gelatin is a collagen-derived biomaterial containing functional groups that can support cell adhesion and provide extracellular-matrix-related cues (Jia et al. 2024; Waidi et al. 2024). Polyvinyl alcohol (PVA) is a hydrophilic polymer that can increase water affinity and reduce the apparent hydrophobicity of PDMS (Carranza et al. 2023). A combined gelatin-PVA coating could therefore provide complementary functions: gelatin could promote cell-surface interaction, while PVA could improve surface wettability (Miranda et al. 2021; Longoni et al. 2023). Nevertheless, the suitability of a coating for a proposed comparative renal platform should be assessed using both cancerous and non-cancerous cell models, rather than a single cell type (Mieville et al. 2023; Wang et al. 2023).

A498 renal carcinoma cells were selected to represent the cancerous condition, while HEK-293 cells were used as a non-RCC, renal-derived comparison model for preliminary material compatibility and plate-based drug response studies(Wolf et al. 2020; Shapiro et al. 2022). Because HEK-293 cells are transformed and do not fully reproduce healthy adult renal epithelium(Somova

et al. 2024; Twardowska et al. 2025), their use was limited to comparative proof-of-concept evaluation. Future studies using primary renal epithelial cells or well-characterized proximal tubular epithelial models will be required to improve the physiological relevance (Telang et al. 2024; Petit et al. 2025). The study therefore focused on three linked steps: screening gelatin-, PVA-, and gelatin-PVA-modified PDMS surfaces; translating the selected coating to a three-channel PDMS device and performing preliminary A498 cell loading; and establishing plate-based 5-FU and HCQ response baselines for future on-chip studies. The overall scope was proof-of-concept development of a renal cell-compatible microfluidic biointerface, with the remaining translational limitations discussed in Section 3.9.

2. Experimental Section

2.1 Materials

Poly(dimethylsiloxane) (PDMS; Sylgard™ 184 Silicone Elastomer Kit) was used to fabricate the microfluidic device and to prepare PDMS substrates for surface-modification studies. The PDMS elastomer base and curing agent were mixed at a mass ratio of 10:1. Polyvinyl alcohol (PVA; average molecular weight approximately 100,000 g mol^{-1}, 80% hydrolyzed, Sigma-Aldrich, India) and gelatin derived from porcine skin (Sigma-Aldrich) were used for surface modification. PVA and gelatin solutions were prepared at concentrations of 10% and 2% (w/v), respectively. For the combined coating, the prepared PVA and gelatin solutions were mixed at a 1:1 volume ratio, corresponding to nominal final concentrations of 5% (w/v) PVA and 1% (w/v) gelatin in the mixed coating solution.

Dulbecco's modified Eagle's medium (DMEM), fetal bovine serum (FBS), phosphate-buffered saline (PBS), trypsin-ethylenediaminetetraacetic acid, and penicillin-streptomycin were obtained from Sigma-Aldrich (Merck Life Science Pvt. Ltd., India). Calcein acetoxymethyl ester (Calcein AM; C1359-100UL) was obtained from Sigma-Aldrich, whereas propidium iodide (P3566) was obtained from Thermo Fisher Scientific. 5-Fluorouracil (5-FU) and hydroxychloroquine (HCQ) were obtained from TCI Chemicals. Dimethyl sulfoxide (DMSO; Sigma-Aldrich) was used to prepare the drug stock solutions. Milli-Q water was used to prepare aqueous solutions.

2.2 Cell lines and maintenance

A498 human renal cell carcinoma cells were used to represent the cancerous renal condition. HEK-293 cells were used as a non-RCC renal-derived comparison cell line. A498 cells between passages 18 and 23 and HEK-293 cells between passages 11 and 16 were used throughout the plate-based experiments. Both cell lines were cultured separately in DMEM supplemented with 10% (v/v) FBS and 1% (v/v) penicillin-streptomycin. The cells were maintained at 37 °C in a humidified incubator containing 5% CO_2. The culture medium was replaced every 2 days. At the 80% confluency, the cells were washed with PBS, detached using trypsin-ethylenediaminetetraacetic acid, and collected for subsequent experiments. A498 and HEK-293 cells were evaluated independently during surface-compatibility and plate-based drug-response experiments. Only A498 cells were introduced into the fabricated microfluidic device. Simultaneous A498 and HEK-293 culture was not performed inside the device.

2.3 Design of the microfluidic platform

A three-channel PDMS microfluidic platform was designed as a proof-of-concept device for the future integration of cancerous and non-cancerous renal cell conditions. The device consisted of two lateral microchannels and one central microchannel. The lateral channels were designed as separate culture regions for future integration of A498 and non-cancerous renal-derived cells, whereas the central channel was designed for controlled delivery of culture medium or therapeutic agents. The assembled device had approximate external dimensions of 50 mm × 40 mm × 20 mm. The microchannels were approximately 700 µm wide and 150 µm deep. The device was designed with three stacked layers. The bottom layer contained the inlet-channel geometry, the middle layer contained the bifurcated channel region, and the top layer contained the outlet-channel geometry. This arrangement was used to create spatially separated regions within the device while maintaining optical access for microscopic observation and enabling controlled fluid movement through the channel network. The device was developed as the material and engineering foundation of a future dual-state renal platform. Comparative culture of the cancerous and non-RCC renal-derived cell models and multidrug testing were not performed inside the device during the present study.

2.4 Fabrication of the PDMS microfluidic device

The PDMS elastomer base and curing agent were mixed at a mass ratio of 10:1. The mixture was stirred thoroughly and degassed under vacuum to remove entrapped air bubbles. The degassed PDMS mixture was poured onto the molds corresponding to the individual device layers and cured in a hot-air oven at 60 °C for 60 min.

After curing, the PDMS layers were carefully separated from the molds. Inlet and outlet openings were created in the upper layer using a biopsy punch of 1 mm. The individual layers were aligned with the designed channel geometry and sequentially bonded to form the complete microfluidic device. The layers were bonded using the oxygen plasma bonding method, and the curing agent was also spread between the layers. They were then left to cure for 10 minutes for permanent bonding.

The assembled device was inspected using an optical microscope (Leica, Inverted Microscope) to confirm layer alignment, channel connectivity, and the absence of visible structural defects. Flexible tubing was connected to the inlet and outlet ports for fluid delivery.

2.5 Qualitative flow visualization and leakage testing

The fabricated device was tested for channel continuity and visible leakage using an aqueous food-color dye. The dye solution was introduced through the inlet ports using a Harvard Syringe Pump 11 Elite Series at a flow rate of 10 µl/min. Flow through the straight channels, bifurcations, junctions, and outlet regions was observed under bright-field microscopy. During the test, the device was checked for incomplete channel filling, visible blockage, fluid leakage, separation between the PDMS layers, and any structural damage. Continuous dye flow from the inlet to the outlet, without visible leakage, was taken as qualitative confirmation that the channels were properly connected and that the bonded layers remained intact. This test provided qualitative validation of channel continuity and visible leakage. In addition, the nominal hydrodynamic conditions associated with the imposed flow rate were estimated analytically as described below. Spatial velocity and pressure distributions were not experimentally measured.

2.6 Analytical estimation of microfluidic flow parameters

Nominal hydrodynamic parameters were estimated from the imposed volumetric flow rate and the reported rectangular-channel dimensions. The channel width (w) and height (h) were 700 and 150 µm, respectively, and the imposed volumetric flow rate (Q) was 10 µL min^{-1} (1.67×10^{-10} m^3 s^{-1}).

For the analytical estimates, the culture medium was treated as an incompressible Newtonian fluid with density $\rho \sim 1000$ kg m^{-3} and dynamic viscosity $\mu = 0.93$ mPa s. The viscosity value was selected from the literature for DMEM supplemented with 10% FBS at 37 °C (Šints et al. 2025). Because serum-supplemented media can exhibit non-Newtonian behavior under some conditions, the calculated values were interpreted as nominal engineering estimates rather than direct measurements of the local flow field.

Cross-sectional area

The rectangular-channel cross-sectional area was calculated as:

$$A = wh$$

where w and h represented channel width and height, respectively

$$A = (700\ x10^{-6})(150\ x10^{-6})$$

$$A = 1.05\ x\ 10^{-7}\ m^2$$

Mean Velocity

The nominal mean fluid velocity was calculated from:

$$U = \frac{Q}{A}$$

$$U = \frac{1.67\ x\ 10^{-10}}{1.05\ x\ 10^{-7}}$$

$$U = 1.59\ mms^{-1}$$

Hydraulic diameter

The hydraulic diameter of the rectangular microchannel was calculated as:

$$D_h = \frac{2wh}{w + h}$$

$$D = 247\ \mu m$$

Reynolds number

The Reynolds number was calculated as:

$$Re = \frac{\rho U D_h}{\mu}$$

$$Re\ \approx 0.42$$

Wall Shear Stress

For the straight-channel regions, nominal wall shear stress was estimated using the rectangular-channel approximation:

$$\tau_w = \frac{6\mu Q}{wh^2}$$

$$\tau_w \approx 0.059\ Pa$$

$$\tau_w \approx 0.59\ dyn\ cm^{-2}$$

2.7 Preparation of PDMS substrates for surface modification

PDMS substrates were prepared in 96-well culture plates for preliminary wettability and biological-compatibility studies. Untreated PDMS substrates were used as the unmodified reference. Three coating conditions were evaluated:

- 2% (w/v) gelatin;
- 10% (w/v) PVA;
- gelatin-PVA prepared at a 1:1 volume ratio.

The gelatin and PVA solutions were prepared separately using Mili-Q water. The dissolution temperature was 60 °C, and the solution was mixed for 60 minutes or until homogeneous. For each coating condition, approximately 100 µL of the coating solution was added to the PDMS-containing wells. The substrates were incubated for 24 h inside a CO_2 incubator. Excess coating material was then removed, and the substrates were washed three times with PBS.

Untreated and modified PDMS substrates were subsequently used for contact angle measurements and plate-based cell compatibility assessment.

2.8 Contact-angle measurement

The surface wettability of untreated and modified PDMS substrates was evaluated using the sessile-droplet method. Measurements were performed on untreated PDMS, gelatin-coated PDMS, PVA-coated PDMS, and gelatin-PVA-coated PDMS.

A 20µL droplet of Milli-Q water was deposited onto each surface using a micropipette. Images of the droplet profile were acquired using a contact-angle goniometer (Kruss-DSA30). A total of 7 droplets were measured on each specimen, and 3 independently prepared specimens were tested for every surface condition. A lower apparent contact angle was interpreted as improved surface wettability. The coating condition that showed the greatest improvement in wettability while retaining favorable cellular compatibility was selected for application within the microfluidic device.

2.9 Plate-based evaluation of cell compatibility

A498 and HEK-293 cells were used separately to evaluate the compatibility of untreated and modified PDMS surfaces. Cells were seeded onto standard tissue-culture wells, untreated PDMS, gelatin-coated PDMS, PVA-coated PDMS, and gelatin-PVA-coated PDMS at a density of 10,000 cells per well. The cultures were maintained under standard conditions at 37 °C and 5% CO_2.

Cell attachment, spreading, aggregation, monolayer formation, and morphological alterations were examined after 24 and 48 hours using an Invitrogen™ FLoid™ Cell Imaging Station. Representative images were acquired from 5 randomly selected fields per sample.

Cellular metabolic activity was assessed using the MTT assay. Briefly, an MTT solution (2.5mg/mL stock solution) was added to each well and incubated for 4 hours at 37 °C. The culture medium was removed, and the resulting formazan crystals were dissolved in DMSO. Absorbance was measured at 570 nm using a microplate reader (Tecan plate reader). Cell viability was normalized to that of cells maintained in standard tissue-culture wells or the stated control condition. The combined coating was selected based on contact angle reduction, cellular morphology, attachment, and MTT-based metabolic activity in both A498 and HEK-293 cells.

2.10 Surface modification of the microfluidic channels

The gelatin-PVA coating was selected for application inside the microfluidic device based on the plate-based wettability and cell-compatibility results. Before coating, the assembled device was sterilized under UV light and rinsed with sterile PBS.

The gelatin-PVA solution was introduced into the microchannels at a flow rate of 10 µL/min, maintained within the channels for 6 hrs at 37 °C, and then kept under static conditions for 18 hrs. Excess coating solution was removed, and the channels were washed 1 times with sterile PBS. Complete culture medium was subsequently introduced before cell loading.

2.11 Preliminary loading of A498 cells into the device

A498 cells were harvested and suspended in complete DMEM at a concentration of approximately 20,000 cells mL^{-1}. The cell suspension was loaded into a sterile syringe and introduced into the gelatin-PVA-coated microfluidic channels via a syringe pump at a flow rate of 10 µL/min. Following cell introduction, the device was maintained under static conditions for approximately

12 h to promote preliminary cell attachment to the channel surfaces. The complete culture medium was then added, and the cells were maintained for 5 days. The presence and spatial distribution of A498 cells within the channels were examined using bright-field microscopy. Qualitative live/dead fluorescence imaging was also performed using Calcein AM and propidium iodide to visualize viable and membrane-compromised cells, respectively. The fluorescence images were interpreted qualitatively; cell attachment efficiency, proliferation, phenotype, and drug response were not quantified inside the device.

2.12 Plate-based drug-response experiments

All drug-response experiments were conducted under plate-based culture conditions. No drug treatment was performed inside the fabricated microfluidic device.

A498 and HEK-293 cells were seeded separately into a 96-well format at a density of 10,000 cells per well and incubated for 24 and 48 hours. Stock solutions of 5-FU and HCQ were prepared at 10 mM in DMSO. The stock solutions were diluted with complete culture medium to obtain final concentrations of 5, 10, 20, 40, 80, and 160 μM. Cells were treated with 5-FU or HCQ for 24 and 48 h. Cellular morphology after treatment was examined using an inverted microscope. Cell metabolic activity was quantified using the MTT assay as described in Section 2.8. The drug-response measurements obtained in plate culture were used as baseline data for future translation to the proposed dual-state microfluidic platform.

2.13 Calculation of cell viability and half-maximal inhibitory concentration

Cell viability was calculated from the MTT absorbance measurements using:

$$\text{Cell viability}(\%) = \frac{A_{Treated} - A_{blank}}{A_{control} - A_{blank}} x\ 100$$

Where $A_{treated}$ was the absorbance measured for the drug-treated group, A_{contol} was the absorbance measured for the control, and A_{blank} was the background absorbance measured in wells without cells.

For the quantitative potency comparison presented in this study, the half-maximal inhibitory concentration (IC50) was estimated from the 48 h normalized viability data by fitting a four-parameter logistic concentration-response model using GraphPad Prism. The fitted IC_{50} values and corresponding 95% confidence intervals were obtained for each drug-cell line combination. When

valid (IC_{50}) values were available for both A498 and HEK-293 cells under the same experimental conditions, the plate-based selectivity index was calculated as:

$$\text{Selectivity Index (SI)} = \frac{IC50_{HEK\ 293}}{IC50_{A498}}$$

The selectivity index was interpreted only as an in vitro plate-based comparison and not as evidence of on-chip therapeutic selectivity.

2.14 Statistical analysis

All quantitative experiments were performed using three independent replicates unless otherwise stated, and data are presented as mean ± standard deviation (SD). Statistical analyses were performed using Origin software. Differences among surface-treatment conditions were analyzed using one-way analysis of variance (ANOVA) followed by Dunnett's multiple-comparison test, with the standard 2D tissue-culture condition used as the control. A value of $p < 0.05$ was considered statistically significant.

3. Results and Discussion

3.1 Fabrication and fluidic validation of the three-channel microfluidic platform

A three-channel poly(dimethylsiloxane) microfluidic platform was fabricated as a proof-of-concept system for the future comparative evaluation of responses in cancerous and non-cancerous renal cells (Nishimura 2024). The device was composed of three patterned PDMS layers that contained the inlet, bifurcated middle, and outlet channel geometries, respectively (Fig. 1.). After alignment and bonding, two lateral channels and one central channel were formed. The lateral channels were designed as separate culture compartments for renal carcinoma and non-RCC renal-derived cells, whereas the central channel was intended for controlled delivery of culture medium or therapeutic agents (Jang and Suh 2010; Jang et al. 2013). The assembled device had approximate external dimensions of 50 mm × 40 mm × 20 mm, and the channels were approximately 700 μm wide and 150 μm deep.

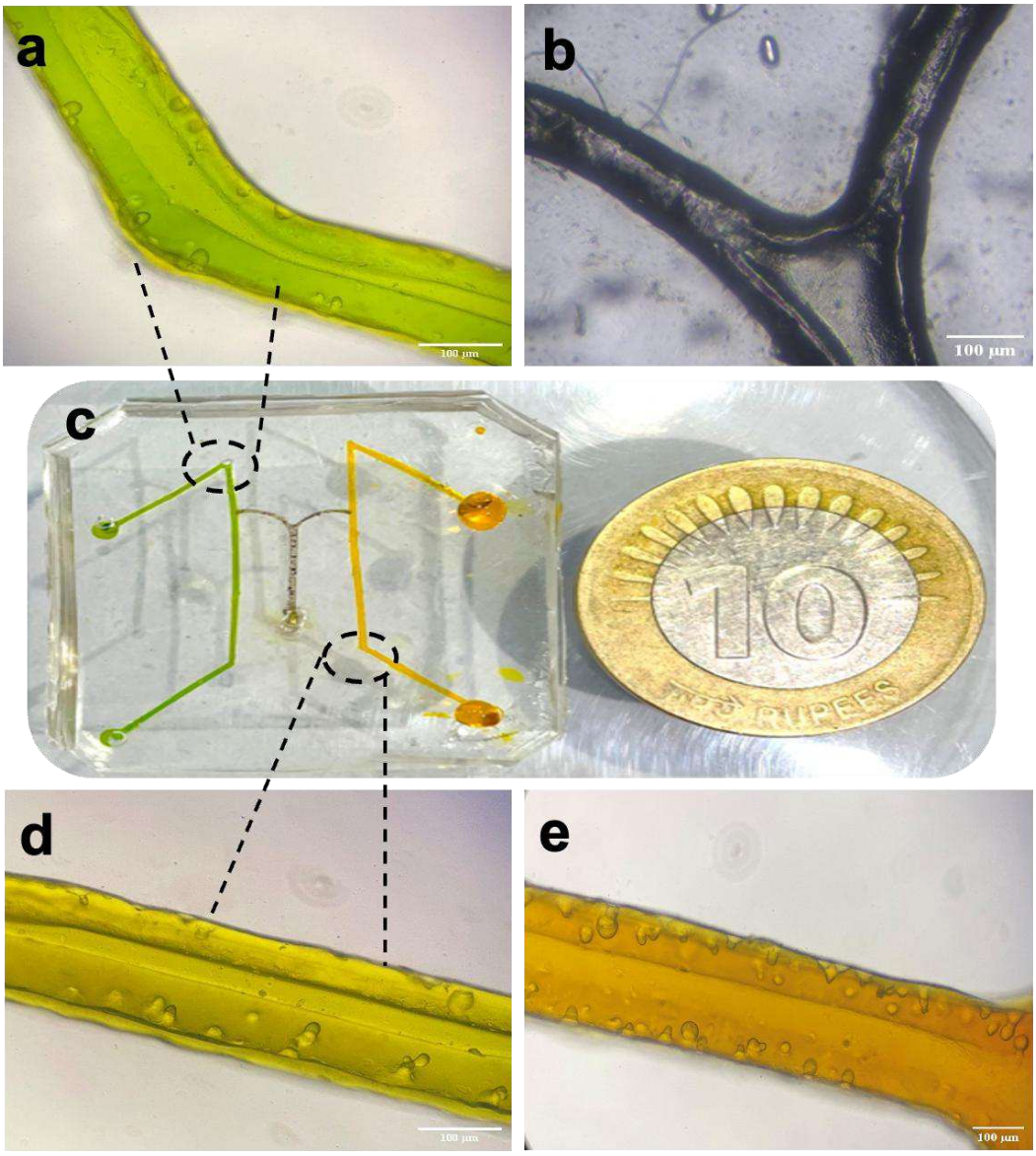


Fig. 2. Qualitative flow visualization and fluidic validation of the fabricated three-channel PDMS microfluidic device. (a) Bright-field microscopy image showing continuous transport of green dye through a curved channel. (b) Enlarged microscopic view of a bifurcation junction, confirming preservation of the designed channel geometry after multilayer assembly. (c) Photograph of the complete microfluidic device after colored dye was introduced through the inlet ports; a 10-rupee coin was included as a scale reference. The marked regions indicate the locations corresponding to the enlarged microscopic views. (d) Microscopic image showing continuous filling of a straight channel section with green dye. (e) Microscopic image showing dye transport through a second channel section. Scale bars =100 µm.

The multilayer structure was formed without visible channel collapse or major deformation. The optical transparency of PDMS enabled direct examination of the alignment of the channel layers and the internal geometry of the assembled device. This property was important because the

proposed platform required repeated microscopic observation of fluid movement and cell distribution within enclosed channels. PDMS has been widely used for microfluidic cell culture systems because it combines optical transparency, flexibility, gas permeability, and compatibility with soft lithographic processing (Miranda et al. 2021).

The fluidic integrity of the fabricated device was assessed using colored aqueous dye. As shown in Fig. 2, the dye entered the microchannel network and passed through the straight sections, bifurcated regions, and outlet channels without visible interruption. Complete filling of the channel network indicated that the separately fabricated layers had been aligned and bonded sufficiently to preserve channel continuity. No visible leakage, layer separation, or fluid accumulation outside the designed channels was observed under the tested condition.

The dye-flow experiment confirmed the device's basic functionality before biological testing. In multilayer microfluidic platforms, incomplete bonding or misalignment may produce leakage, obstruction, or unintended communication between adjacent compartments (Borók et al. 2021). Such defects could alter cell seeding, nutrient delivery, and drug exposure. Therefore, the continuous transport of dye through the fabricated network provided qualitative evidence that the device was suitable for subsequent coating and cell-loading experiments.

The dye-flow images provided direct qualitative evidence of channel connectivity and the absence of visible leakage, while the imposed flow condition was further characterized analytically. For a rectangular channel with a width of 700 μm and a height of 150 μm, the cross-sectional area was 1.05×10^{-7} m², and the hydraulic diameter was approximately 247 μm. At 10 μL min^{-1}, the nominal mean velocity was approximately 1.59 mm s^{-1}. Using $\rho\approx1000$ kg m^{-3} and $\mu=0.93$ mPa.s, the corresponding Reynolds number was approximately 0.42, confirming that the straight-channel regions operated in a low-Reynolds-number laminar-flow regime. The nominal wall shear stress calculated was approximately 0.059 Pa or 0.59 dyn cm^{-2}. These values provided an engineering estimate of the hydrodynamic environment associated with the imposed flow rate (Gande et al. 2024).

The calculated Reynolds number, substantially below unity, indicated that viscous forces dominated over inertial effects within the straight microchannel regions. Such low-Reynolds-number behavior is characteristic of microscale flow and results in predictable pressure-driven transport with limited inertial mixing. The calculated wall shear stress further provided a

quantitative reference for the mechanical environment that would be experienced by surface-attached cells during perfusion.

Table 1: Analytical hydrodynamic characteristics of the microchannel at 10 μL min^{-1}

Parameter	Value
Channel Width, w	700 μm
Channel height, h	150 μm
Flow rate, Q	10 μL min^{-1}
Cross-Sectional area, A	1.05 x10^{-7} m^2
Mean Velocity, U	1.59 mms^{-1}
Hydraulic diameter, D_h	247 μm
Reynolds number, Re	0.42
Wall shear stress, τ_w	0.59yn cm^{-2}

3.2 Modification of PDMS wettability using gelatin and PVA

The inherent hydrophobicity of untreated PDMS was evaluated by measuring the apparent contact angle with water. As shown in Fig. 3, untreated PDMS exhibited a contact angle of approximately 115°, which confirmed poor interaction between the native surface and the aqueous phase. This behavior was consistent with the low surface energy of the methyl groups on PDMS (Miranda et al. 2021; Neves et al. 2024).

A clear reduction in contact angle was observed after surface modification. PVA-coated PDMS showed a contact angle of approximately 82-84°, whereas Gelatin-coated PDMS showed a value of approximately 77°. The combined gelatin-PVA coating produced the lowest measured contact angle of approximately 74°. Therefore, the gelatin-PVA treatment reduced the apparent contact angle by approximately 41° compared with untreated PDMS. The decrease in contact angle demonstrated that the surface characteristics of PDMS were altered by the polymer coatings (Lenhart and Kennedy 2023). Gelatin contains polar functional groups and cell-interactive motifs derived from collagen, which can support cell attachment at the material interface. PVA contains hydroxyl groups that increase water affinity and improve the hydrophilic behavior of polymer surfaces (Jiang et al. 2025). When both materials were combined, the wettability contribution of PVA was complemented by the biologically interactive properties of gelatin. This combination was

expected to provide a more suitable interface for renal cell attachment than untreated PDMS (Joo et al. 2021; Wu et al. 2023).

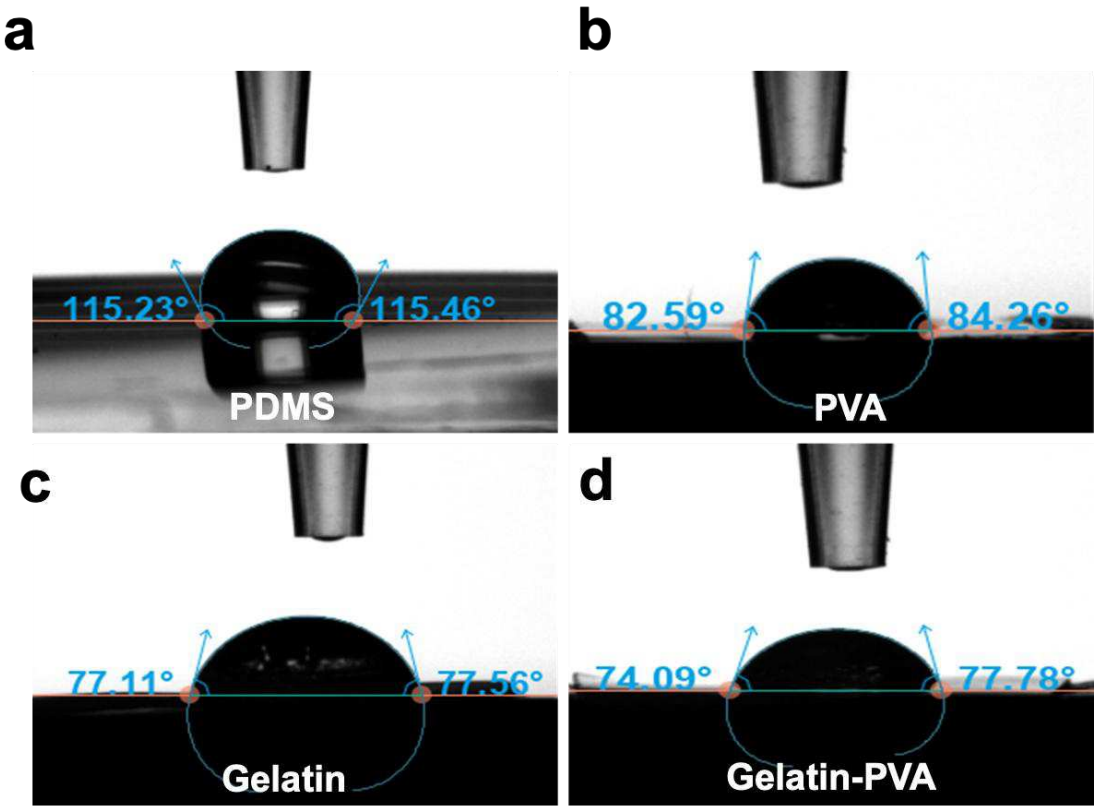


Fig. 3. Apparent water contact-angle analysis of untreated and surface-modified PDMS substrates. Representative sessile water-droplet images were obtained for (a) untreated PDMS, (b) PVA-coated PDMS, (c) gelatin-coated PDMS, and (d) gelatin-PVA-coated PDMS. Untreated PDMS showed the highest apparent contact angle, with left and right measurements of 115.23° and 115.46°, respectively, confirming its hydrophobic surface behavior. Surface modification reduced the apparent contact angle to 82.59° and 84.26° for PVA-coated PDMS, 77.11° and 77.56° for gelatin-coated PDMS, and 74.09° and 77.78° for gelatin-PVA-coated PDMS.

Although the gelatin-PVA condition produced the lowest contact angle, the difference between the PVA and gelatin-PVA coatings was smaller than the difference between either coating and untreated PDMS. Therefore, the combined coating was not selected solely on the basis of contact angle. Its suitability was further evaluated through plate-based morphology and viability studies using A498 and non-RCC renal-derived comparison cells (HEK-293 cells). This combined evaluation was important because improved wettability alone does not necessarily confirm biological compatibility (Hu et al. 2023; Wu et al. 2023).

3.3 Plate-based response of A498 cells to modified PDMS surfaces

The influence of PDMS surface condition on A498 renal carcinoma cells was evaluated through microscopic observation under plate-based culture conditions. As shown in Fig. 4, A498 cells cultured in standard tissue-culture wells exhibited an adherent, well-distributed morphology. On untreated PDMS, cellular attachment was retained, but the distribution was less uniform, and reduced spreading was observed in several regions (Akther et al. 2020; Miranda et al. 2021; Neves et al. 2024). In contrast, cells cultured on gelatin-PVA-coated PDMS showed broader spreading and more continuous surface coverage.

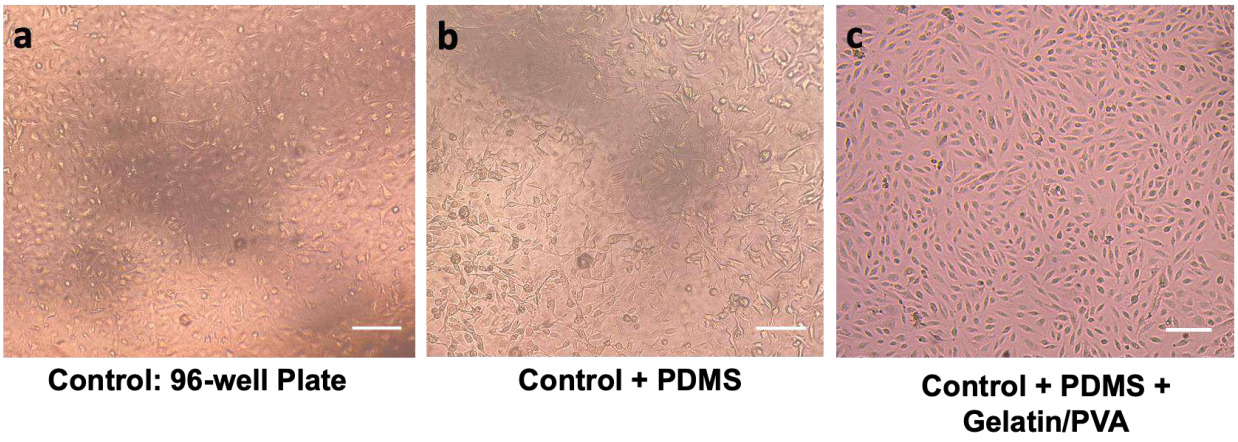


Fig. 4. Plate-based morphological evaluation of A498 renal carcinoma cells on untreated and gelatin-PVA-modified PDMS surfaces. Representative bright-field microscopic images of A498 cells cultured under (a) standard tissue-culture control conditions, (b) untreated PDMS, and (c) gelatin-PVA-coated PDMS. Scale bars = 100 µm.

The improvement in cell morphology corresponded with the decrease in surface hydrophobicity. Highly hydrophobic PDMS can lead to nonuniform wetting and variable adsorption of serum proteins, thereby affecting the formation of an adhesion-supporting interface. After gelatin-PVA modification, increased surface wetting likely enabled more consistent interactions among the culture medium, adsorbed proteins, and the PDMS substrate (Akther et al. 2020; Joo et al. 2021). In addition, gelatin may have provided functional groups that supported cell attachment and spreading (Feng et al. 2026).

A498 cells remained partially adherent even on untreated PDMS, indicating that the adverse effect of native PDMS was not sufficient to prevent cancer-cell attachment completely (Majhy et al.

2021). However, the present study did not examine focal adhesion formation, integrin expression, cytoskeletal organization, or extracellular-matrix signaling. Therefore, the observed difference was attributed only to a surface-dependent change in attachment and spreading, rather than to a specific molecular mechanism. Overall, gelatin-PVA modification provided a more favorable plate-based surface for A498 cells than untreated PDMS. This result was relevant to the proposed application because stable attachment of the cancer-cell compartment would be required before therapeutic exposure could be evaluated in the microfluidic device.

3.4 Plate-based response of non-RCC renal-derived comparison cells to modified PDMS surfaces

A stronger surface-dependent response was observed for non-RCC renal-derived comparison cells (HEK-293 cells). On untreated PDMS, the cells showed limited spreading and formed rounded aggregates or spheroid-like structures (Fig. 5). The formation of aggregates suggested that cell-cell association had been favored when stable attachment to the hydrophobic substrate was limited. In contrast, non-RCC renal-derived comparison cells cultured on gelatin-PVA-coated PDMS showed improved spreading, reduced aggregation, and a more continuous distribution across the surface.

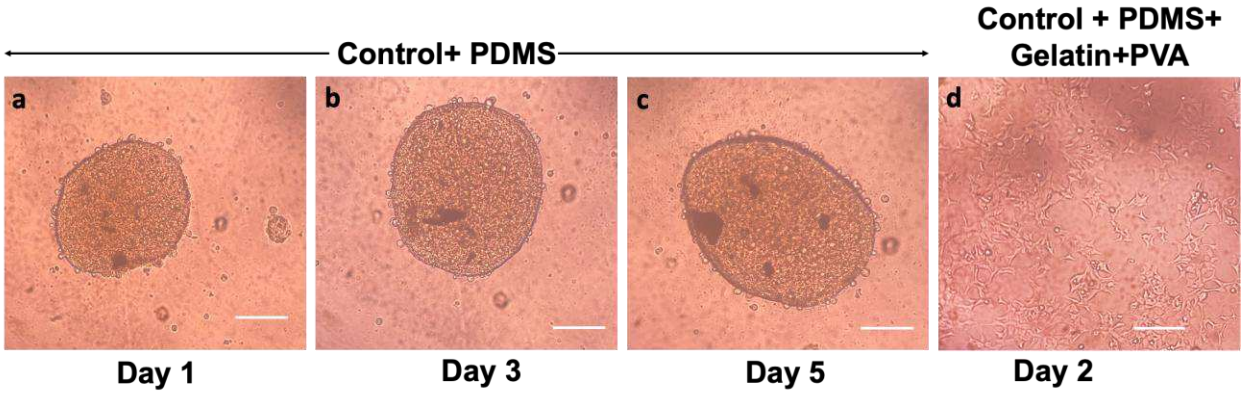


Fig. 5. Plate-based morphological response of non-RCC renal-derived comparison cells to untreated and gelatin-PVA-modified PDMS surfaces. Representative bright-field microscopic images of non-RCC renal-derived comparison cells (HEK-293 cells) cultured on untreated PDMS for (a) 1 day, (b) 3 days, and (c) 5 days, and on (d) gelatin-PVA-coated PDMS. Scale bars = 100 μm.

The response of non-RCC renal-derived comparison cells supported the need for surface modification prior to the development of the proposed dual-state platform. Since both cancerous

and non-cancerous comparison conditions were intended to be integrated within the same PDMS device, a coating suitable only for A498 cells would not have been sufficient. The improved morphological response of both cell models on gelatin-PVA-coated PDMS indicated that the combined coating provided a more generally compatible surface (Zhang et al. 2022; Wu et al. 2023).

The difference between the A498 and HEK-293 responses also demonstrated that a material's biological performance cannot be inferred from a single cell type. A498 cells retained some attachment on untreated PDMS, whereas non-RCC renal-derived comparison cells showed more pronounced rounding and aggregation. These findings indicated that surface compatibility depended on both the characteristics of the cell model and the material surface (Zhang et al. 2022; Wu et al. 2023).

HEK-293 cells were used as a non-RCC renal-derived comparison cell line. The HEK-293 lineage was established through adenoviral transformation of cells derived from human embryonic kidney tissue and has since undergone extensive adaptation for long-term culture and recombinant protein production (Tan et al. 2021). These transformed characteristics limit its ability to reproduce the differentiated transport, polarity, and functional phenotype of healthy adult renal epithelial cells. Current kidney-modeling studies therefore increasingly use primary proximal tubular epithelial cells, induced pluripotent stem cell-derived renal cells, organoids, or organ-on-chip models to model physiological renal function (Nguyen et al. 2023; Musah et al. 2024). Accordingly, the present findings were interpreted as preliminary evidence of surface compatibility. Future validation should incorporate a more physiologically representative renal epithelial model before normal-versus-cancer drug responses are compared inside the device.

3.5 Cell metabolic activity on untreated and modified PDMS

The effect of surface modification on cellular metabolic activity was evaluated using the MTT assay (Fig. 6). The normalized metabolic activity was lowest on untreated PDMS (78.67 ± 2.70%) and increased after surface modification. Gelatin-coated PDMS showed a metabolic activity of 91.37 ± 2.23%, while PVA-coated PDMS showed a value of 81.93 ± 4.14%. The highest response among the modified PDMS conditions was observed for the gelatin-PVA coating, reaching 97.17 ± 1.62% and approaching the response of the 2D tissue-culture control. A significant difference was observed among the tested surface conditions (one-way ANOVA, $F(4,10) = 40.57$, $p <$

0.0001). Dunnett's multiple-comparison test, using the 2D tissue-culture condition as the reference, showed that metabolic activity was significantly lower on untreated PDMS ($p < 0.0001$), gelatin-coated PDMS ($p = 0.0063$), and PVA-coated PDMS ($p < 0.0001$). In contrast, no significant difference was observed between gelatin-PVA-coated PDMS and the 2D control ($p = 0.487$). These results indicated that the combined gelatin-PVA coating elicited a cellular metabolic response most similar to that observed under standard tissue-culture conditions.

The MTT results were consistent with the contact-angle and morphological observations. Untreated PDMS exhibited the highest apparent contact angle and showed the least favorable cellular response. Following surface modification, improved wettability was accompanied by better cell spreading and increased metabolic activity. Similar relationships between improved PDMS wettability and enhanced cell attachment or biological response have been reported following hydrophilic surface modification (Miranda et al. 2021; Neves et al. 2024). However, wettability alone does not determine cellular behavior, as surface chemistry, protein adsorption, coating composition, and cell-specific characteristics can also influence attachment and metabolic activity(Zhang et al. 2022; Wu et al. 2023).

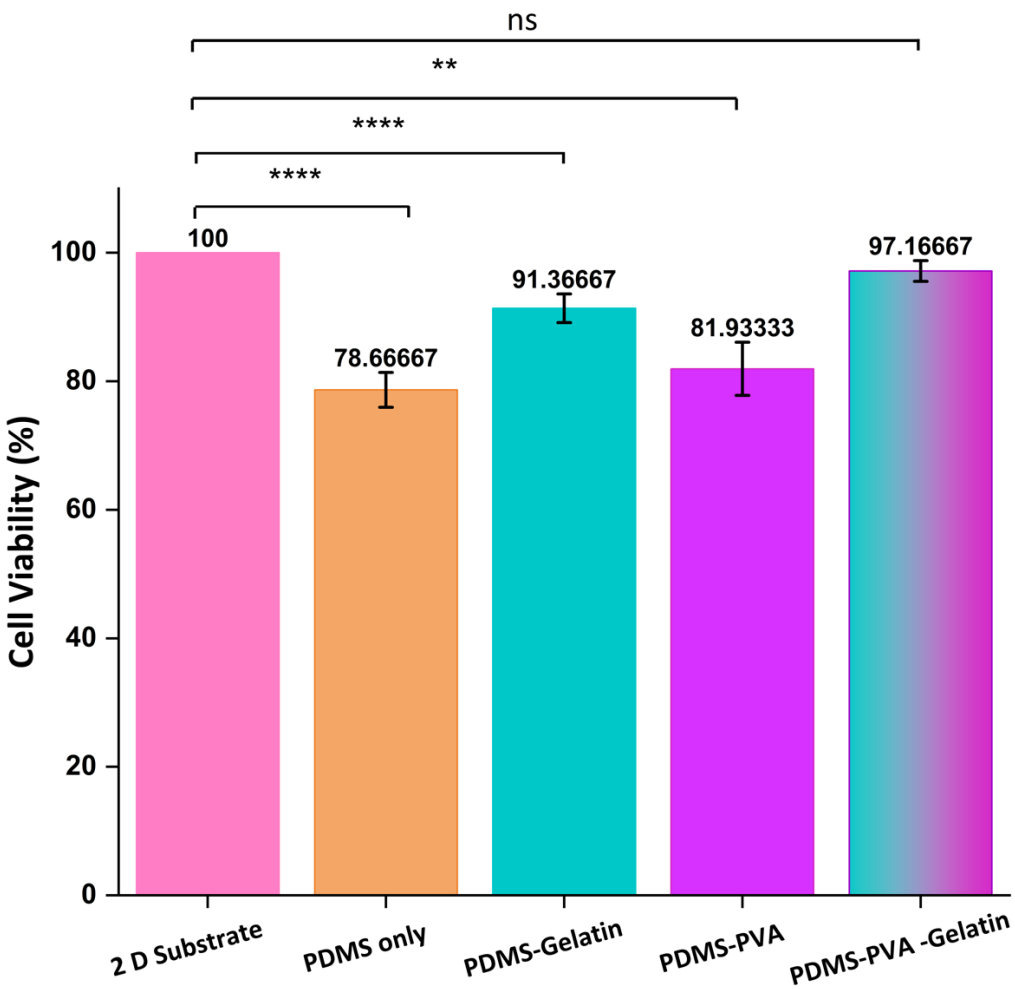


Fig. 6. MTT-based metabolic activity of cells cultured under standard 2D tissue-culture conditions and on untreated PDMS, gelatin-coated PDMS, PVA-coated PDMS, and gelatin-PVA-coated PDMS. Data are presented as mean ± SD (n = 3). Statistical differences were analyzed by one-way ANOVA, followed by Dunnett's multiple-comparison test, with the 2D tissue-culture condition as the control. Metabolic activity was significantly lower on untreated PDMS, gelatin-coated PDMS, and PVA-coated PDMS compared with the 2D control, whereas no significant difference was observed for gelatin-PVA-coated PDMS. **$p < 0.01$, ****$p < 0.0001$; ns, not significant.

The MTT assay is based on the reduction of tetrazolium salt to formazan by cellular oxidoreductase activity. Therefore, the measured absorbance was interpreted as an indicator of cellular metabolic activity rather than as a direct measurement of cell number, proliferation, or absolute viability (Ghasemi et al. 2021; Hoogstraten et al. 2022). Differences in the MTT signal may arise from changes in cell attachment, cell density, mitochondrial activity, cellular stress, or metabolic state. For this reason, the MTT findings were considered alongside the microscopic morphology and

surface wettability results rather than used as a standalone measure of biological compatibility(Riss et al. 2016; Ghasemi et al. 2021; Hoogstraten et al. 2022).

The agreement among contact-angle measurements, microscopic morphology, and MTT-based metabolic activity strengthened the conclusion that surface modification improved the biological usability of PDMS. Gelatin-PVA was selected as the most suitable coating because it combined the lowest measured apparent contact angle with favorable attachment, spreading, and metabolic activity in both A498 and HEK-293 cultures. This integrated selection approach reduced the likelihood of identifying a coating based solely on a single material or biological parameter. Nevertheless, the MTT results were obtained under plate-based conditions, and equivalent cellular performance inside the coated microchannels remains to be established.

3.6 Selection of gelatin-PVA coating for microfluidic device integration

The surface-screening experiments established a connected material-selection pathway. Native PDMS exhibited poor wettability and a less favorable cellular response, whereas gelatin and PVA modifications improved the surface's interaction with the aqueous culture environment. The combined gelatin-PVA coating produced the lowest apparent contact angle among the tested conditions and supported favorable morphological and metabolic responses in both A498 and HEK-293 cells. Surface modification of PDMS is commonly required for biological microfluidic applications because native PDMS is hydrophobic, and the effectiveness of a modification strategy depends not only on reducing the contact angle but also on its ability to support the intended biological interaction (Miranda et al. 2021; Neves et al. 2024).

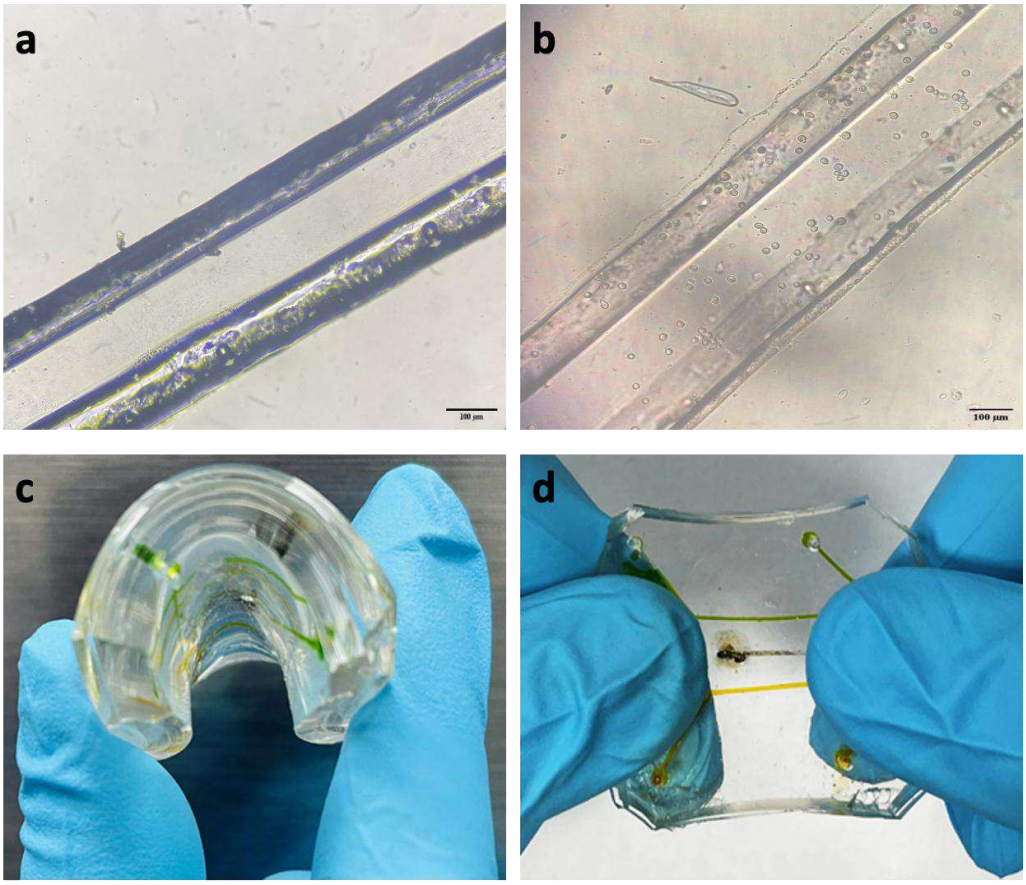


Fig.7. Representative microscopic and macroscopic images showing the fabricated PDMS-based microfluidic device and its mechanical flexibility. (a) Microscopic image of the empty microchannel showing the channel boundaries and internal flow region. (b) Microscopic image of cells introduced into the microchannel, showing their distribution within the confined channel space. (c) Photograph of the fabricated device under bending, demonstrating the flexible nature of the PDMS structure without visible cracking or delamination. (d) Photograph of the device under manual stretching, demonstrating its ability to withstand deformation while maintaining the microfluidic platform's overall structural integrity. Scale bars in (a) and (b) are 100 µm.

The gelatin-PVA coating was therefore selected to modify the internal surfaces of the microfluidic device. This selection was based on the combined material and biological findings rather than on wettability alone. PVA contributes hydrophilic hydroxyl groups that improve water affinity, while gelatin provides a collagen-derived, biologically interactive component that can support cell attachment (Feng et al. 2026). Recent studies on PVA/gelatin-based biomaterials have similarly shown that combining these polymers can provide favorable wettability and improved cellular interactions, making the blend useful for biomaterial interfaces intended for cell culture applications (Wu et al. 2023; Batool et al. 2024).

The use of a common coating was particularly relevant to the intended dual-state platform because the two lateral channels were designed to contain biologically different renal cell conditions while being fabricated from the same PDMS substrate. Applying the same surface treatment to both culture compartments could reduce material-related variability between the cancerous and non-cancerous conditions and allow future differences in cellular response to be interpreted primarily in relation to the cell model and therapeutic exposure rather than to differences in the underlying substrate.

However, the coating behavior inside the enclosed microchannels was not quantitatively characterized in the present study. The coating thickness, uniformity, surface chemistry, and stability under continuous flow were not examined in the present study. This is an important limitation because a coating that performs well on a flat PDMS surface may not behave in the same way inside a confined microchannel. Factors such as coating deposition, washing steps, fluid shear, and prolonged exposure to culture medium can affect how well the coating remains attached to the channel surface and how consistently it supports cell growth. Previous studies on PDMS surface modification have therefore highlighted the need to evaluate coating stability and cell attachment under actual microchannel and flow conditions rather than relying only on static planar-surface testing (Akther et al. 2020; Neves et al. 2024). Gelatin-based coatings have been successfully used to support cell attachment in PDMS channels, but their performance can still depend on the coating method and the applied flow conditions.

For this reason, the plate-based findings were used only as preliminary evidence for selecting gelatin-PVA as the most suitable coating for device integration. They did not confirm that the coating would show the same behavior inside the microchannels. Future work should therefore examine coating uniformity, its retention after sterilization and perfusion, and the ability of cells to remain attached under controlled flow before establishing simultaneous culture of cancerous and non-cancerous renal cells.

3.7 Preliminary loading of A498 cells into the coated microfluidic device

Following the selection of the gelatin-PVA coating, A498 cells were introduced into the modified microfluidic device to check whether the cells could be successfully loaded into the channels. Microscopic observation confirmed the presence of cells within selected regions of the device (Fig. 8). Because PDMS is optically transparent, cells can be observed directly within the channels

without opening or disturbing the device, which is a useful feature of PDMS-based microfluidic systems (Miranda et al. 2021; Neves et al. 2024).

This experiment linked the earlier plate-based surface studies with the fabricated microfluidic platform. The successful loading of A498 cells showed that the selected coating procedure, device design, and cell-loading method could be used together at a preliminary stage. Previous microfluidic studies have also reported that gelatin-containing surface coatings can support cell attachment and improve cell retention within microchannels during culture and flow exposure (Akther et al. 2020; Sato et al. 2023). The presence of gelatin in the coating may have further supported cell-surface interactions through its collagen-derived adhesion-related components, while the improved wettability of the modified PDMS facilitated the cell suspension spreading more easily along the channel surface (Akther et al. 2020).

The bright-field and fluorescence observations provided preliminary evidence that A498 cells could be introduced into and maintained within the gelatin-PVA-coated device. Calcein-positive fluorescence was visible in the representative fields, whereas no visible propidium iodide signal was observed in the corresponding images (Fig. 8), suggesting that the imaged cells remained predominantly viable under the tested static culture condition. This assessment remained qualitative because neither live nor dead cells were counted, and attachment efficiency, proliferation, spatial coverage, and phenotypic stability were not quantitatively assessed. The images, therefore, supported preliminary on-chip cytocompatibility but did not establish long-term performance under continuous perfusion. The analytically estimated nominal wall shear stress corresponding to a flow rate of 10 μL min^{-1} was approximately 0.059 Pa. However, the cells were initially maintained under static conditions to allow attachment, and cell retention under continuous exposure to this nominal shear condition was not quantitatively evaluated. Therefore, the calculated shear stress was interpreted as a physical descriptor of the imposed flow condition rather than as evidence of cellular tolerance to continuous perfusion.

Therefore, further studies will be required to determine whether the loaded cells remain attached and maintain suitable viability and morphology after flow is introduced and during longer-term culture. In microfluidic culture systems, cell retention and morphology can be influenced by surface coating, seeding density, incubation time before flow initiation, and the magnitude of fluid-induced shear stress (Akter et al. 2021; Sasaki et al. 2022; Sato et al. 2023). Accordingly, the

present observations were interpreted only as preliminary evidence that A498 cells could be introduced into and visualized within the gelatin-PVA-coated device.

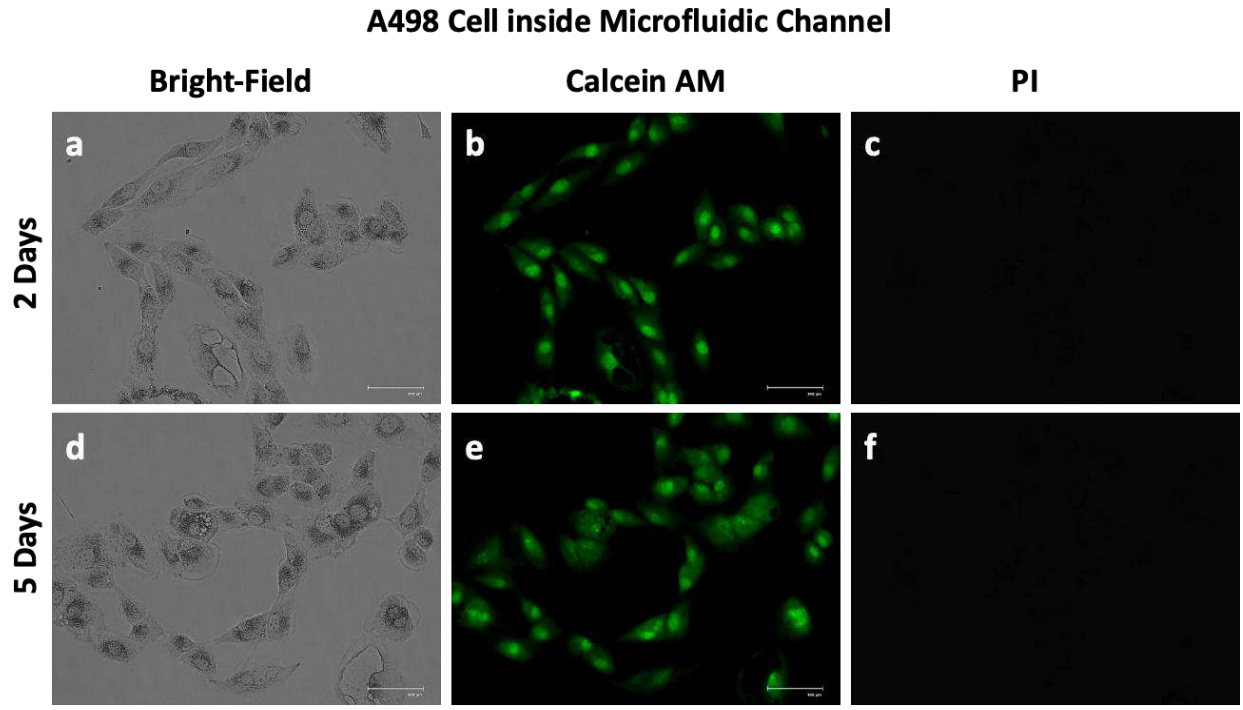


Fig. 8. Representative bright-field and fluorescence micrographs of A498 renal carcinoma cells cultured within the gelatin-PVA-modified PDMS microfluidic device. Bright-field images in panels (a) and (d) show the distribution and morphology of cells within the microchannels. Calcein AM-positive fluorescence in panels (b) and (e) indicates metabolically active cells, whereas no visible propidium iodide fluorescence was observed in the corresponding representative fields shown in panels (c) and (f). The staining was evaluated qualitatively and was not used for quantitative viability analysis. Scale bars = 100 μm.

The next stage of platform validation should therefore determine whether A498 cells remain attached after flow initiation and whether their viability, morphology, and proliferation are maintained during extended culture. Quantitative live/dead analysis, cell-covered area, attachment retention, and temporal monitoring under controlled perfusion would provide stronger evidence of biological compatibility. Such characterization will be necessary before the device can be extended to simultaneous cultures of cancerous and non-cancerous renal cells and comparative on-chip drug evaluation.

3.8 Plate-based drug response to 5-fluorouracil and hydroxychloroquine

Drug-response experiments were performed under plate-based culture conditions and were not conducted inside the microfluidic device. These experiments were carried out to establish

preliminary drug-sensitivity profiles of cancerous and non-RCC renal-derived comparison cells prior to future translation to the proposed dual-state microfluidic platform.

Untreated A498 cells retained an adherent morphology and relatively high confluence. Following exposure to 5-fluorouracil (5-FU) or hydroxychloroquine (HCQ), reduced cell attachment, cellular contraction, decreased confluence, and increased cellular debris were observed. These morphological alterations became more pronounced after 48 h than after 24 h, indicating an exposure-time-dependent increase in treatment-associated cellular damage.

A498 cells showed greater sensitivity to 5-FU than to HCQ under the tested conditions. The quantitative potency comparison reported here was based on the 48 h dose-response data. At 48 h, the estimated IC50 values were 14.6 μM for 5-FU and 60.4 μM for HCQ in A498 cells. In comparison, HEK-293 cells showed IC50 values of 65.37 μM for 5-FU and 104.60 μM for HCQ. Thus, a substantially lower concentration of 5-FU was required to reduce A498 metabolic activity by 50% than was required for HCQ, while the higher IC50 values in HEK-293 cells indicated lower sensitivity of the non-RCC renal-derived comparison cells under the same plate-based exposure conditions.

The different responses to the two compounds were consistent with their distinct mechanisms of action. 5-FU is a fluoropyrimidine antimetabolite that is metabolically converted into active intracellular derivatives. These metabolites inhibit thymidylate synthase and interfere with DNA and RNA synthesis, thereby disrupting nucleic-acid metabolism and suppressing cell proliferation (Ghafouri-Fard et al. 2021; dos Santos et al. 2022). HCQ acts through a different mechanism and has been widely investigated as an autophagy-modulating compound in cancer. Its accumulation in acidic intracellular compartments interferes with lysosomal function and autophagic processing, including autophagosome-lysosome fusion. However, the anticancer response to HCQ varies according to cell type, concentration, treatment duration, and dependence of the cells on autophagic pathways (Ferreira et al. 2021; Jain et al. 2023). The stronger inhibitory response to 5-FU observed in the present study was therefore consistent with its direct antiproliferative mechanism, although thymidylate synthase activity, autophagic flux, apoptosis, and other pathway-specific molecular markers were not experimentally evaluated.

The selectivity analysis further distinguished the response of the two compounds. Based on the 48 h IC_{50} values, 5-FU showed a selectivity index of 4.48, whereas HCQ showed a lower selectivity index of 1.73. Selectivity indices, based on the ratio of the IC_{50} in a non-cancerous cell model to

that in a cancer cell model, are commonly used as an initial measure of preferential anticancer activity, with values above 1 indicating greater inhibitory activity toward the cancer cell model relative to the comparison cells (Tronina et al. 2023).

Table 2. Plate-based 48 h dose-response parameters for A498 and HEK-293 cells treated with 5-fluorouracil and hydroxychloroquine.

Drug	Cell Model	IC50(μM)	Selectivity Index
5-Fluorouracil (5-FU)	A498	14.6	4.48
5-Fluorouracil (5-FU)	HEK-293	65.37	-
Hydroxychloroquine (HCQ)	A498	60.4	1.73
Hydroxychloroquine (HCQ)	HEK-293	104.60	-

The higher SI observed for 5-FU indicated that A498 cells were approximately 4.5-fold more sensitive than HEK-293 cells, based on their respective IC_{50} values. In comparison, the SI of 1.73 for HCQ indicated a smaller difference in sensitivity between the two cell models. Therefore, among the two tested compounds, 5-FU showed the more favorable in vitro selectivity profile, combining a lower IC_{50} toward A498 cells with a greater separation between the A498 and HEK-293 responses. HCQ also showed preferential inhibition of A498 cells relative to HEK-293 cells, but its lower SI indicated comparatively limited selectivity under the tested conditions. The SI values were interpreted only within the present experimental conditions, because selectivity depends on the cancer and comparison cell models used, as well as the assay conditions and exposure period. Recent in vitro studies have similarly used the ratio of non-cancer-cell IC_{50} to cancer-cell IC_{50} to distinguish compounds with preferential anticancer activity (Perużyńska et al. 2021; Tronina et al. 2023).

The selectivity analysis was particularly relevant to the intended purpose of the proposed dual-state microfluidic platform. Evaluation of A498 cells alone would provide information on anticancer activity but would not indicate whether a similar drug concentration also affected the non-RCC comparison condition. The parallel A498 and HEK-293 measurements therefore provided a preliminary indication of the balance between cancer-cell inhibition and potential toxicity toward the comparison cells. However, HEK-293 cells are transformed renal-derived cells

and were not regarded as equivalent to normal adult renal epithelium. Accordingly, the calculated SI values represented preliminary comparative indices rather than definitive measures of renal therapeutic safety.

The plate-based drug-response experiments also did not demonstrate the drug-screening capability of the fabricated microfluidic device. Translation of these concentrations directly to a PDMS-based microfluidic system requires additional characterization because PDMS can absorb or adsorb small

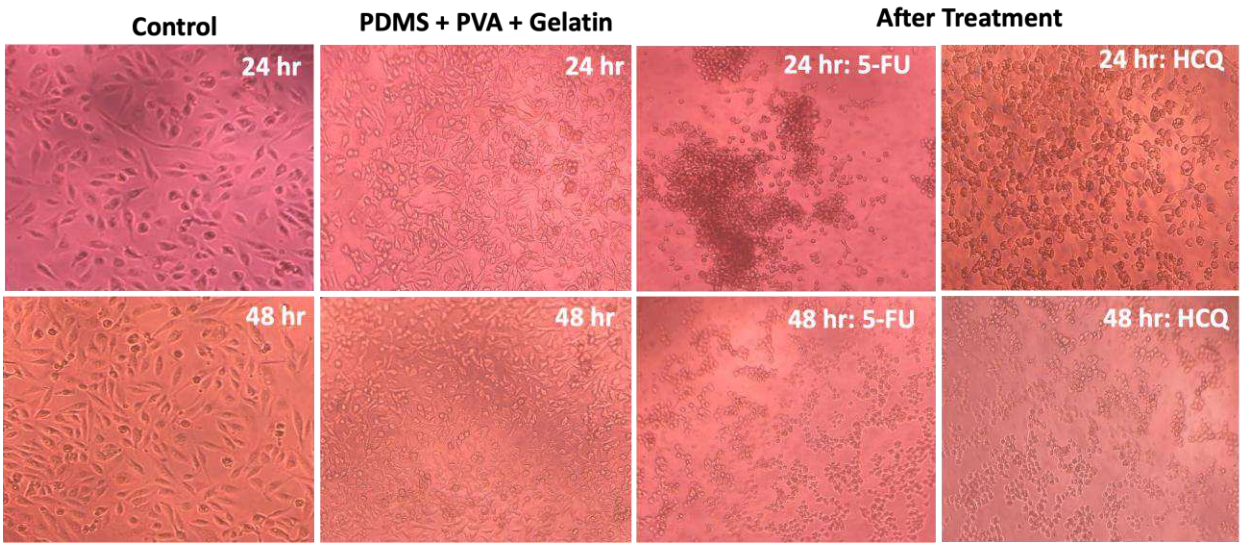


Fig. 9. Representative phase-contrast microscopic images showing the morphological response of cultured A498 cells under untreated and drug-treated conditions after 24 and 48 h. The upper row presents the cellular morphology after 24 h, while the lower row shows the corresponding observations after 48 h. The untreated groups showed attached and well-spread cells, with an increase in cell density over time. In contrast, cells treated with 5-fluorouracil (5-FU) and hydroxychloroquine (HCQ) showed reduced spreading, loss of the typical adherent morphology, increased cell rounding, and partial detachment from the culture surface. These morphological changes became more evident after 48 h, indicating a time-dependent cellular response to both drug treatments.

molecules, particularly compounds with physicochemical properties that favor partitioning into the polymer. Such interactions can alter the effective drug concentration reaching cells and generate spatial and temporal differences between the nominally administered concentration and the concentration actually present within a microchannel (Grant et al. 2021). Grant et al. demonstrated that drug transport in PDMS organ-chip systems is governed by a combination of absorption, adsorption, convection, and diffusion, emphasizing the importance of determining effective drug exposure when quantitative pharmacological responses are evaluated in PDMS devices (Grant et al. 2021).

Accordingly, the present drug-response results were considered a plate-based baseline for future translation rather than evidence of on-chip therapeutic performance. Future studies should determine the effective concentrations of 5-FU and HCQ within the coated device, establish cellular retention and viability under perfusion, and compare dose-response behavior between the cancerous and non-cancerous compartments under identical flow and exposure conditions. Incorporation of a more physiologically representative renal epithelial cell model would further strengthen the biological relevance of the selectivity assessment. Such an approach would allow the proposed platform to evaluate not only the inhibitory effect of a therapeutic compound on renal carcinoma cells but also its relative effect on the non-cancerous renal condition within the same microfluidic environment.

3.9 Scope and Significance

The principal contribution of this study was the development of a gelatin-polyvinyl alcohol (gelatin-PVA)-modified polydimethylsiloxane (PDMS) microfluidic platform for renal cell culture applications. A compartmentalized three-channel microfluidic architecture was fabricated and integrated with a surface-modification strategy to improve the wettability and biological compatibility of PDMS. The surface properties of untreated and modified PDMS were systematically evaluated using contact angle measurements, cellular morphology, and metabolic activity analysis. Based on these evaluations, the gelatin-PVA coating was selected and subsequently applied to the microfluidic channels. The fluidic functionality of the fabricated device was demonstrated through qualitative dye-flow visualization, while analytical hydrodynamic calculations were performed to characterize the low-Reynolds-number flow regime and estimate the nominal wall shear stress. Furthermore, A498 renal carcinoma cells were successfully introduced into the modified microchannels, and their preliminary cellular compatibility was demonstrated through bright-field and fluorescence imaging. Comparative plate-based drug-response experiments involving 5-fluorouracil (5-FU) and hydroxychloroquine (HCQ) were also performed to establish baseline therapeutic responses in renal-derived cell models. Thus, these findings established the feasibility of integrating polymer-based surface engineering, controlled microfluidic architecture, and renal cell culture within a single experimental platform. The developed system provided a foundation for subsequent investigations

of cellular responses under controlled fluidic conditions and the development of comparative renal drug-evaluation platforms.

4. Conclusions

A gelatin-polyvinyl alcohol-modified poly(dimethylsiloxane) microfluidic platform was developed as a proof-of-concept system for renal cell culture and future comparative therapeutic evaluation. The three-channel device was successfully fabricated using a multilayer PDMS architecture, and dye-flow testing confirmed continuous channel filling without visible leakage. Surface modification reduced the hydrophobicity of native PDMS, with the gelatin-PVA coating producing the lowest representative apparent water contact angle among the evaluated conditions. Plate-based studies further showed that the modified surfaces supported more favorable attachment, spreading, and metabolic activity of A498 renal carcinoma and HEK-293 renal-derived comparison cells than untreated PDMS.

Based on the combined wettability and biological compatibility results, the gelatin-PVA coating was selected for modifying the microfluidic channels. At the reported channel dimensions and a flow rate of 10 μL min^{-1}, analytical calculations yielded a mean velocity of approximately 1.59 mm s^{-1}, a hydraulic diameter of approximately 247 μm, a Reynolds number of approximately 0.42, and a nominal wall shear stress of approximately 0.059 Pa. These values established that the straight-channel regions operated in a low-Reynolds-number laminar-flow regime and provided a quantitative reference for the physical microenvironment. A498 cells were subsequently introduced into the coated device, and representative Calcein AM/propidium iodide images qualitatively indicated viable cells within the microchannels. Plate-based exposure to 5-fluorouracil and hydroxychloroquine produced distinct drug-dependent responses, with 5-fluorouracil showing the stronger inhibitory effect on A498 cells under the evaluated conditions.

The present study did not establish simultaneous A498 and non-RCC renal-derived comparison cells or comparative drug testing inside the device. It should therefore be regarded as a materials and device development study rather than a fully validated renal cancer-on-a-chip model. Within this scope, the combination of surface wettability, plate-based cell compatibility, qualitative on-chip A498 cytocompatibility, baseline comparative drug response, and analytical microfluidic characterization established a more complete material-fluidic-biological foundation for subsequent comparative renal drug-evaluation studies.

Data availability: All data analyzed during this study are included in this manuscript.

Declarations: There are no conflicts to declare.

Acknowledgments: UG sincerely acknowledges the financial assistance of the Indian Institute of Technology (IIT) Jammu, India. The authors also acknowledge the Central Instrumentation Facility for providing the necessary research infrastructure.

Reference:

Akter S, Habib A, Islam MA, et al (2021) Comprehensive performance assessment of deep learning models in early prediction and risk identification of chronic kidney disease. IEEE Access 9:165184-165206

Akther F, Yakob SB, Nguyen N-T, Ta HT (2020) Surface modification techniques for endothelial cell seeding in PDMS microfluidic devices. Biosensors 10:182

Barré-Sinoussi F, Montagutelli X (2015) Animal models are essential to biological research: issues and perspectives. Future Sci OA 1 (4): FSO63

Batool S, Liaqat U, Hussain Z (2024) Preparation and physicochemical characterization of whitlockite/PVA/Gelatin composite for bone tissue regeneration. Front Chem 12:1355545

Borók A, Laboda K, Bonyár A (2021) PDMS bonding technologies for microfluidic applications: A review. Biosensors 11:292

Carranza T, Uranga J, Irastorza A, et al (2023) Combination of 3D printing and electrospinning to develop chitin/gelatin/PVA scaffolds. Int J Bioprinting 9:701

Chumbimuni-Torres KY, Coronado RE, Mfuh AM, et al (2011) Adsorption of proteins to thin-films of PDMS and its effect on the adhesion of human endothelial cells. RSC Adv 1:706-714

Das A, Prajapati P (2025) Navigating pharmaceuticals: Microfluidic devices in analytical and formulation sciences. Discov Chem 2:49

Das U, Kamble A, Mandal S, et al (2026) Unveiling the Best Fit: Comparative Perspective on Animal Models Used for Chronic Diseases. SN Compr Clin Med 8:254

DesRochers TM, Palma E, Kaplan DL (2014) Tissue-engineered kidney disease models. Adv Drug Deliv Rev 69:67-80

dos Santos AM, Junior AGT, Carvalho SG, Chorilli M (2022) An updated review on properties, nanodelivery systems, and analytical methods for the determination of 5-fluorouracil in pharmaceutical and biological samples. Curr Pharm Des 28:1501-1512

Feng C, Chen M, Qu D-H (2026) Physically Cross-Linked Hydrogels Based on Poly (vinyl alcohol) and Gelatin for Independent Modulation of Mechanical Cues in Cell Adhesion Studies. ACS Appl Bio Mater 9:3029-3037

Ferreira PMP, de Sousa RWR, de Oliveira Ferreira JR, et al (2021) Chloroquine and hydroxychloroquine in antitumor therapies based on autophagy-related mechanisms.

Pharmacol Res 168:105582

Gande VV, Podupu PKR, Berry B, et al (2024) Engineering advancements in microfluidic systems for enhanced mixing at low Reynolds numbers. Biomicrofluidics 18:

Ghafouri-Fard S, Abak A, Tondro Anamag F, et al (2021) 5-Fluorouracil: a narrative review on the role of regulatory mechanisms in driving resistance to this chemotherapeutic agent. Front Oncol 11:658636

Ghasemi M, Turnbull T, Sebastian S, Kempson I (2021) The MTT assay: utility, limitations, pitfalls, and interpretation in bulk and single-cell analysis. Int J Mol Sci 22:12827

Gokaltun A, Yarmush ML, Asatekin A, Usta OB (2017) Recent advances in nonbiofouling PDMS surface modification strategies applicable to microfluidic technology. Technology 5:1-12

Grant J, Özkan A, Oh C, et al (2021) Simulating drug concentrations in PDMS microfluidic organ chips. Lab Chip 21:3509-3519

Hoogstraten CA, Smeitink JAM, Russel FGM, Schirris TJJ (2022) Dissecting drug-induced cytotoxicity and metabolic dysfunction in conditionally immortalized human proximal tubule cells. Front Toxicol 4:842396

Hu X, Wang T, Li F, Mao X (2023) Surface modifications of biomaterials in different applied fields. RSC Adv 13:20495-20511

Jain V, Singh MP, Amaravadi RK (2023) Recent advances in targeting autophagy in cancer. Trends Pharmacol Sci 44:290-302

Jang K-J, Mehr AP, Hamilton GA, et al (2013) Human kidney proximal tubule-on-a-chip for drug transport and nephrotoxicity assessment. Integr Biol 5:1119-1129

Jang K-J, Suh K-Y (2010) A multi-layer microfluidic device for efficient culture and analysis of renal tubular cells. Lab Chip 10:36-42

Jia X, Fan X, Chen C, et al (2024) Chemical and structural engineering of gelatin-based delivery systems for therapeutic applications: a review. Biomacromolecules 25:564-589

Jiang Y, Ayaz Z, Xiang L, et al (2025) Sodium carboxymethylcellulose/polydopamine biocellulose coatings with enhanced wet stability for implantable medical devices. ACS Appl Bio Mater 8:1050-1064

Joo H, Park J, Sutthiwanjampa C, et al (2021) Surface coating with hyaluronic acid-gelatin-crosslinked hydrogel on gelatin-conjugated poly (dimethylsiloxane) for implantable medical

device-induced fibrosis. Pharmaceutics 13:269

Kaur N, Savitsky MJ, Scutte A, et al (2025) Navigating cancer treatment: A journey from 2D to 3D cancer models and nanoscale therapies. ACS Pharmacol Transl Sci 8:3773-3800

Lenhart AE, Kennedy RT (2023) Evaluation of surface treatments of PDMS microfluidic devices for improving small-molecule recovery with application to monitoring metabolites secreted from islets of Langerhans. ACS Meas Sci au 3:380

Lima RA (2025) The impact of polydimethylsiloxane (PDMS) in engineering: recent advances and applications. Fluids 10:41

Longoni A, Major GS, Jiang S, et al (2023) Pristine gelatin incorporation as a strategy to enhance the biofunctionality of poly (vinyl alcohol)-based hydrogels for tissue engineering applications. Biomater Sci 12:134-150

Majhy B, Priyadarshini P, Sen AK (2021) Effect of surface energy and roughness on cell adhesion and growth-facile surface modification for enhanced cell culture. RSC Adv 11:15467-15476

McDonald JC, Whitesides GM (2002) Poly (dimethylsiloxane) as a material for fabricating microfluidic devices. Acc Chem Res 35:491-499

Mieville V, Griffioen AW, Benamran D, Nowak-Sliwinska P (2023) Advanced in vitro models for renal cell carcinoma therapy design. Biochim Biophys Acta (BBA)-Reviews Cancer 1878:188942

Miranda I, Souza A, Sousa P, et al (2021) Properties and applications of PDMS for biomedical engineering: A review. J Funct Biomater 13:2

Mirlohi MS, Akar S, Yazdani K, et al (2026) Microfluidic platforms for precision delivery of therapeutic cells in regenerative and personalized medicine. Adv Drug Deliv Rev 234:115865

Musah S, Bhattacharya R, Himmelfarb J (2024) Kidney disease modeling with organoids and organs-on-chips. Annu Rev Biomed Eng 26:

Neves LB, Afonso IS, Nobrega G, et al (2024) A review of methods to modify the PDMS surface wettability and their applications. Micromachines 15:670

Nguyen VVT, Gkouzioti V, Maass C, et al (2023) A systematic review of kidney-on-a-chip-based models to study human renal (patho-) physiology. Dis Model Mech 16:dmm050113

Nishimura Y (2024) Revolutionizing renal research: The future of kidney-on-a-chip in

biotechnology. Regen Ther 26:275-280

Perużyńska M, Borzyszkowska-Ledwig A, Sośnicki JG, et al (2021) Synthesis and Anticancer Activity of Mitotic-Specific 3, 4-Dihydropyridine-2 (1 H)-thiones. Int J Mol Sci 22:2462

Petit I, Faucher Q, Bernard J-S, et al (2025) Proximal tubule-on-chip as a model for predicting cation transport and drug transporter dynamics. Sci Rep 15:2580

Riss TL, Moravec RA, Niles AL, et al (2016) Cell viability assays. Assay Guid Man [Internet]

Sasaki S, Suzuki T, Morikawa K, et al (2022) Fabrication of a gelatin-based microdevice for vascular cell culture. Micromachines 14:107

Sato Y, Yamamoto H, Kato H, et al (2023) Microfluidic cell engineering on high-density microelectrode arrays for assessing structure-function relationships in living neuronal networks. Front Neurosci 16:943310

Shapiro DD, Virumbrales-Muñoz M, Beebe DJ, Abel EJ (2022) Models of renal cell carcinoma used to investigate molecular mechanisms and develop new therapeutics. Front Oncol 12:871252

Šints V, Cīmurs J, Birjukovs M, et al (2025) Physical model of serum supplemented medium flow in organ-on-a-chip systems. PLoS One 20:e0322069

Somova M, Simm S, Padmyastuti A, et al (2024) Integrating tumor and healthy epithelium in a micro-physiology multi-compartment approach to study renal cell carcinoma pathophysiology. Sci Rep 14:9357

Soo JY-C, Jansen J, Masereeuw R, Little MH (2018) Advances in predictive in vitro models of drug-induced nephrotoxicity. Nat Rev Nephrol 14:378-393

Tan E, Chin CSH, Lim ZFS, Ng SK (2021) HEK293 cell line as a platform to produce recombinant proteins and viral vectors. Front Bioeng Biotechnol 9:796991

Telang AC, Ference-Salo JT, McElliott MC, et al (2024) Sustained alterations in proximal tubule gene expression in primary culture associate with HNF4A loss. Sci Rep 14:22927

Tronina T, Bartmańska A, Popłoński J, et al (2023) Prenylated flavonoids with selective toxicity against human cancers. Int J Mol Sci 24:7408

Twardowska M, Łyskowski A, Misiorek M, et al (2025) Human embryonic kidney HEK293 cells as a model to study SMVT-independent transport of biotin and biotin-furnished nanoparticles in targeted therapy. Int J Mol Sci 26:1594

Waidi YO, Kariim I, Datta S (2024) Bioprinting of gelatin-based materials for orthopedic

application. Front Bioeng Biotechnol 12:1357460

Wang H, Shi X, Cao X, et al (2023) Discrimination between human normal renal tissue and renal cell carcinoma by dielectric properties using in-vitro BIA. Front Physiol 14:1121599

Wolf MM, Kimryn Rathmell W, Beckermann KE (2020) Modeling clear cell renal cell carcinoma and therapeutic implications. Oncogene 39:3413-3426

Wu I-C, Liou J-W, Yang C-H, et al (2023) Self-assembly of gelatin and collagen in the polyvinyl alcohol substrate and its influence on cell adhesion, proliferation, shape, spreading and differentiation. Front Bioeng Biotechnol 11:1193849

Zhang R, Zhang D, Sun X, et al (2022) Polyvinyl alcohol/gelatin hydrogels regulate cell adhesion and chromatin accessibility. Int J Biol Macromol 219:672-684

Zhang X, Liu A, Wang Y, et al (2025) Advancements and future perspectives of microfluidic technology in pediatric healthcare. Smart Med 4:e70018

Zhang Y, Payab N, Weigelin B, Schürch CM (2026) From 2D cultures to 3D systems: evolving cancer models at the interface of functional precision medicine and theranostics. Theranostics 16:4042